buildings

MDPI

Article

Performance of Rubberized Concrete and the Effect of Temperature and Stainless Steel Fibers

Ayman El-Zohairy *, Matthew Sanchez, Bahram Abediniangerabi and Perry Moler

Department of Engineering and Technology, Texas A&M University-Commerce, Commerce, TX 75429, USA
* Correspondence: ayman.elzohairy@tamuc.edu; Tel.: +1-903-468-8683

Abstract: Rubberized concrete is widely used in construction by utilizing the advantages of partially replacing fine or coarse aggregate with rubber to enhance several properties of concrete and provide an environmentally friendly solution. This paper experimentally explores the influence of utilizing crumb rubber (CR) as an alternate coarse aggregate in concrete. Concrete specimens were prepared with different percentages of rubber (0%, 5%, 10%, 15%, and 20%). Additionally, other parameters, such as freezing–thawing cycles, temperature, and stainless steel fibers (SSFs), were investigated. The workability of fresh concrete and the compression properties of hardened concrete were examined. Reductions in the mechanical properties of rubberized concrete were obtained. The compressive strength reductions ranged between 13% and 50%, based on the percentage of CR in the concrete mix. However, a lesser unit weight and higher toughness were obtained relative to conventional concrete. The average unit weight decreased by 1.3%, 2.5%, 3.4%, and 5.7% of the control mixture when 5%, 10%, 15%, and 20% of the CR were incorporated into the concrete mixtures, respectively. Regression models to predict the compressive strength and unit weight of concrete with CR were developed. In addition, a life cycle cost analysis (LCCA) to identify and quantify the possible benefits of using CR in concrete mixes was carried out. Using rubberized concrete mixtures for thin whitetopping offered a slightly lower net present value compared to the ordinary concrete mix.

Keywords: rubberized concrete; crumb rubber; mechanical properties; stainless steel fibers; mode of failure; life cycle cost analysis

check for updates

Citation: El-Zohairy, A.; Sanchez, M.; Abediniangerabi, B.; Moler, P. Performance of Rubberized Concrete and the Effect of Temperature and Stainless Steel Fibers. *Buildings* **2023**, *13*, 280. https://doi.org/10.3390/buildings13020280

Academic Editor: Elena Ferretti

Received: 1 December 2022
Revised: 11 January 2023
Accepted: 16 January 2023
Published: 18 January 2023

Copyright: © 2023 by the authors. Licensee MDPI, Basel, Switzerland. This article is an open access article distributed under the terms and conditions of the Creative Commons Attribution (CC BY) license (https://creativecommons.org/licenses/by/4.0/).

1. Introduction

Approximately 300 million waste tires are discarded in the USA every year and added to the current tires stockpiled around the country [1]. The removal of rubbers from used tires is the most eco-friendly issue, unless they are recycled in an environmental way [2]. Recently, 35% of waste tires have been recycled, 50% of them have been reused to make tire-derived fuels, and the remainder (15%) have been decomposed or burned in landfills [3]. A possible environmentally friendly approach to recycling waste tires instead of burning or burying them in landfills is to re-use the rubber content existing in the tires as partial replacements of the fine or coarse aggregates in concrete after passing through some chemical and mechanical processes. Nowadays, rubberized concrete is considered one of the most important green concrete materials produced by replacing natural aggregates with rubber particles from old tires in a concrete mixture [4].

Previous researchers have studied the impact of adding waste rubber aggregates as substitutes on the mechanical properties of concrete. The lower unit weight for crumb rubber (CR) provides a better choice to be a lightweight substitute for natural aggregates [5]. Concrete blends with different dosages of shredded or crumbed rubber were prepared to investigate their impact on the mechanical properties of concrete. Rubberized concrete exhibited reductions in workability as the rubber content increased [6]. Concrete mixes with CR were more workable than concrete mixes with coarse tire rubber [7]. However, the test results conducted by Padhi and Panda [8] indicated that as the fine rubber quantity

increased, the workability of both conventional and self-compacting rubberized concrete decreased. The use of rubberized concrete for certain structural members was limited due to reductions in compressive strength [9]. The corresponding ultimate strain increased due to the effect of rubber [10]. The lower adhesiveness of the rubberized aggregate and cement paste was the main reason for this reduction in strength. The rubber-cement matrix interface was found to play a major role in controlling the macro-mechanical properties of rubberized concrete [11,12]. A higher strength was developed when finer-sized rubber particles were used [13]. However, coarse and medium rubber sizes in concrete show more workability relative to concrete with fine rubber sizes [14]. The content ratio of rubber controlled the reductions in the tensile strength of concrete [15,16]. The utilization of silica fume in rubberized concrete enhanced corrosion behavior and decreased corrosion current density values [17].

The reduction in the mechanical properties can be compensated for by adding steel fibers to the rubberized concrete mix [18,19]. For conventional concrete, the flexural toughness increased significantly when steel fibers were added, which plays an important role in enhancing tensile and flexural strength by transforming concrete from a brittle material to a semi-ductile material [20]. Steel fibers improved the fracture energy, toughness, and shrinkage deformation of rubberized concrete [21].

Previous studies were found concerning the effect of environmental conditions, such as temperature and freezing–thawing cycles, on concrete [22,23]. Exposure to elevated temperatures causes additional reductions in the residual mechanical properties of rubberized concrete [24,25]. Analytical models have been proposed to predict these residual properties [26]. The thermal conductivity of rubberized concrete is strongly affected by temperature due to porosity changes and water loss [10]. This conductivity degrades as the rubber particle size decreases or the rubber content increases. The efficacy of CR in providing freezing–thawing resistance in concrete was investigated [27]. The strengthening effect due to steel fibers vanished under the effect of freezing–thawing cycles [28].

The mechanical properties of rubberized concrete have been widely investigated in previous studies. However, more experimental investigations are still needed at different ages and under the effects of different parameters to develop regression models to predict the compressive strength and unit weight of concrete with CR. Moreover, the long-term economic potential of implementing rubberized concrete is not well known and needs to be explored. Therefore, concrete specimens were prepared with different percentages of rubber (0%, 5%, 10%, 15%, and 20%) and tested at different ages. Additionally, other parameters, such as freezing–thawing cycles, temperature, and stainless steel fibers (SSFs), were investigated. The workability of fresh concrete and the compression properties of hardened concrete were examined. Regression models to predict the compressive strength and unit weight of concrete with CR were developed. Moreover, the long-term economic potentials of implementing rubberized concrete were explored by presenting a life cycle cost analysis (LCCA) to identify and quantify the possible benefits of using CR in concrete mixes.

2. Experimental Setup

Five rubberized concrete mixes, as listed in Table 1, were designed to prepare 195 concrete cylinders and 45 concrete prisms. Different percentages of rubber (0%, 5%, 10%, 15%, and 20%) were used. Concrete without CR acted as the reference mix. The workability of fresh concrete and the compression properties of hardened concrete (i.e., unit weight, stress–strain relationships, compressive strength, modulus of elasticity, compression toughness, and tensile strength) were examined.

Table 1. Ratios of the concrete mix ingredients.

Mix	Cement (kg/m^3)	Aggregate		Water (kg/m^3)	Rubber		SSFs (%)
		Sand (kg/m^3)	Gravel (kg/m^3)		Weight (kg/m^3)	Volume (%)	
C-0	464	742	1253	231	0	0	0, 1, and 2
RC-5	464	742	1190	231	36	5	0, 1, and 2
RC-10	464	742	1128	231	73	10	0, 1, and 2
RC-15	464	742	1064	231	108	15	0, 1, and 2
RC-20	464	742	1002	231	144	20	0, 1, and 2

2.1. Materials

2.1.1. Concrete

The concrete mix ratio between cement: fine aggregate: coarse aggregate of the reference mix (C-0) was 1: 1.6: 2.7. The water-to-cement ratio used was 0.5 for all concrete mixes. Ordinary Portland Cement that meets ASTM C150/C150M-20 [29] with a unit weight of 3150 kg/m^3 was used. Sand with a specific gravity of 2.6 was used to prepare the concrete mixes. Gravel interlocks with a nominal maximum size of 10 mm and a specific gravity of 2.65 were utilized. Sieve analyses of the aggregates used were performed, as presented in Figure 1. The rubberized concrete mixtures were made by partially substituting the coarse aggregate with recycled CR. The replacement ratios of rubber used were 5% (RC-5), 10% (RC-10), 15% (RC-15), and 20% (RC-20) of the volume of gravel (see Table 1).

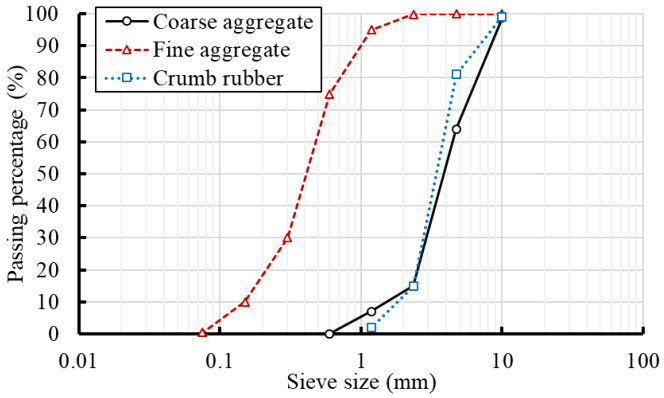

Figure 1. Particle size distributions of the aggregates and the CR.

2.1.2. Crumb Rubber

The size of the particles of the used CR ranged from 3 mm to 6 mm, and the bulk density was 302.5 kg/m^3. Figure 2a shows a sample of the CR aggregates used. The source of the CR aggregate was recycled tires and was provided by Cobalt Holdings, LLC. These tires were manufactured from natural and synthetic rubber along with many chemical additives, including zinc, sulfur, black carbon, and oils that contain polycyclic aromatic hydrocarbons (Cobalt Holdings, LLC.). The sieve analysis of the rubber is presented in Figure 1.

2.1.3. Stainless Steel Fibers (SSFs)

NYCON-SSF TYPE V SSFs, as shown in Figure 2b, were used to reinforce the rubberized concrete. The specific gravity was 7.8. The filament diameter was 1.18 mm, and the length was 38 mm, with an aspect ratio of 32. The tensile strength and modulus of elasticity were 1030 MPa and 203 GPa, respectively.

(**a**) (**b**)

Figure 2. Crumb rubber and stainless steel fibers. (**a**) Crumb rubber. (**b**) Stainless steel fibers.

2.2. Preparation and Curing of Specimens

The concrete ingredients were dry mixed with the CR using a mechanical mixer (see Figure 3), and then water was added gradually. The fresh concrete was mixed for about 4 min until a homogenous mix was obtained. Concrete cylinders of 100 mm × 200 mm and standard prisms of 150 mm × 150 mm × 530 mm were prepared according to ASTM C31/C31M [30]. In the curing process, the concrete cylinders remained in the plastic molds for 24 h. After removal of the concrete specimens, the concrete cylinders and prisms were immersed in water at room temperature for 28 days.

Figure 3. Dry mixing of concrete ingredients with crumb rubber.

2.3. Detection of Temperature, Freezing–Thawing, and Stainless Steel Fiber Effects

The influence of temperature was investigated by storing the designated concrete cylinders under the effects of temperatures: 3 °C, 21 °C, 40 °C, 121 °C, and 260 °C. The concrete cylinders were stored in temperature control ovens (see Figure 4a) at the desired temperature until the day of testing (age of 28 days). On the other hand, the designated specimens were subjected to freezing and thawing cycles at temperatures −3 °C and 21 °C, respectively. Each specimen was exposed to −3 °C for 12 h and then to 21 °C for another 12 h. Each specimen was tested at the age of 28 days after 28 freezing–thawing cycles. The freeze–thaw testing machine is shown in Figure 4b. Moreover, the mechanical behavior of SSF concrete containing CR was explored by manufacturing five concrete mixes to produce concrete cylinders and prisms. The SSFs were added at three-volume ratios of 0%, 1%, and 2%.

(**a**) (**b**)

Figure 4. Temperature control equipment. (**a**) Temperature control ovens. (**b**) Freeze–thaw testing machine.

2.4. Test Set-Up

Compression tests following ASTM C39/C39M–20 [31] were conducted using a standard compression machine, as shown in Figure 5a. This machine was able to capture the stress–strain curves for each specimen by data acquisition. The machine was working under force control with a loading rate of 9 kN/min. The readings of the applied load and axial deflection were recorded during the compression tests by the load cell attached to the machine head plate and the extensometer, respectively. A gauge length of 100 mm and dial gauges of 0.002 mm accuracy were used to calculate the axial strains of the tested concrete cylinders (see Figure 5b). Splitting tensile tests were carried out according to ASTM C496/C496M-17 [32], as illustrated in Figure 5c. The flexural tests were carried out according to ASTM, C293/C293M-16 [33], as presented in Figure 5d. Three tested specimens were implemented for each group of tests, and the average results were adopted.

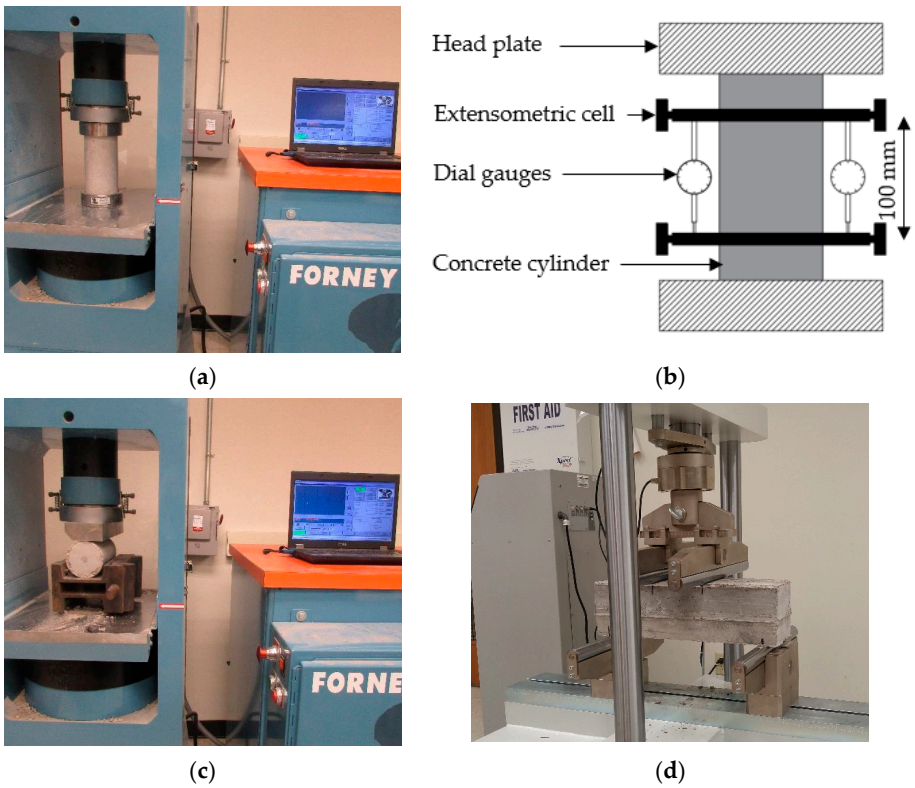

(**a**) (**b**)

(**c**) (**d**)

Figure 5. Types of equipment for compression, splitting, and flexural tests. (**a**) Uniaxial compression tests. (**b**) Axial strain measurements. (**c**) Splitting tests. (**d**) Flexural tests.

3. Test Results and Discussion

The workability of fresh concrete and the compression properties of hardened concrete (i.e., unit weight, compressive strength, modes of failure, modulus of elasticity, toughness, and stress–strain relationships) were examined at different ages of concrete as follows.

3.1. Slump Test Results

Slump tests were achieved according to ASTM C143/C143M-15a [34] to explore the fresh-state behavior of the rubberized concrete mixes. The slump test results were between 95 mm and 260 mm (see Figure 6a). Increasing the CR content caused a reduction in the slump reading. This low workability of rubber-based concrete was due to the hindrance in the movement of concrete ingredients by rubber particles and the lack of adhesion between the cement paste and rubber particles. These results confirmed that the rubber-based concrete mix needs a higher water/cement ratio than normal concrete to coat the CR particles and ensure enough free water to accomplish cement hydration [6]. The percentage slump loss factor is calculated using Equation (1) as follows:

$$\text{Slump loss } \% = \frac{S_o - S_f}{S_o} \times 100 \quad (1)$$

where S_o is the slump of reference mix and S_f is the slump of rubber or SSFs based concrete mix. Additional reductions in the slump were obtained when SSFs were used in the concrete mixes, and these reductions increased as the content of the SSFs increased. When 20% CR content and 0% SSFs were used, the slump reading was reduced by 30%. However, this reduction increased to 45% and 55% when using 1.0% and 2.0% of SSFs, respectively (see Figure 6b). Previous studies confirmed the same trend for the slump values when different percentages of steel fibers and rubber were used [21].

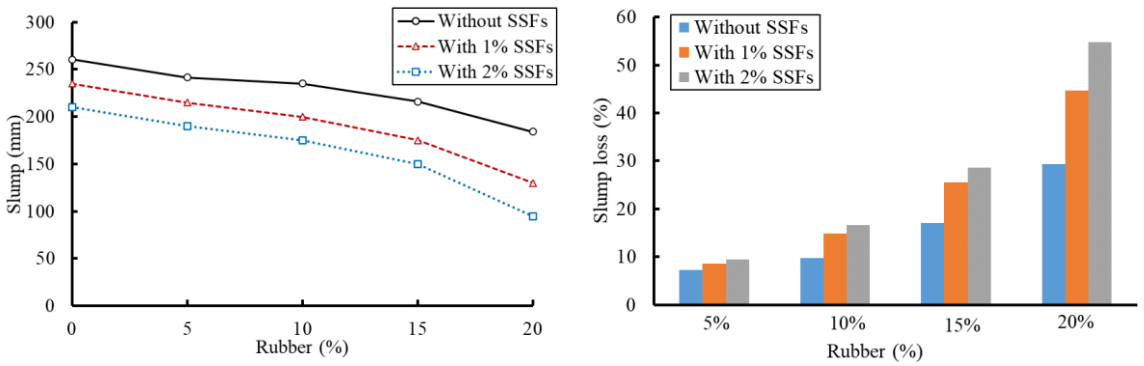

(**a**) (**b**)

Figure 6. Slump test results for all concrete mixes. (**a**) Effect of CR and SSFs on slump test values. (**b**) Percentage of slump loss.

3.2. Unit Weight

In this study, a digital caliper was used to measure the dimensions and subsequently calculate the volume of each specimen. At the same time, a digital scale was used to measure the weight of each cylinder. Based on the weight and volume of each concrete cylinder, the unit weight was determined at the age of 28 days. The effect of CR and SSF replacement ratios on unit weight is illustrated in Figure 7. The average unit weight dropped by 1.3%, 2.5%, 3.4%, and 5.7% of the reference mix when 5%, 10%, 15%, and 20% of the CR content were utilized in the concrete mixtures, respectively. The lower relative unit weight of rubber particles relative to the natural coarse aggregate was the reason for these reductions [35]. At 5% CR content, SSF concrete had an average unit weight of 23.0 kN/m^3 and 23.6 kN/m^3 for SSF content of 1.0% and 2.0%, respectively. These values decreased as the content ratio of CR increased (see Figure 7).

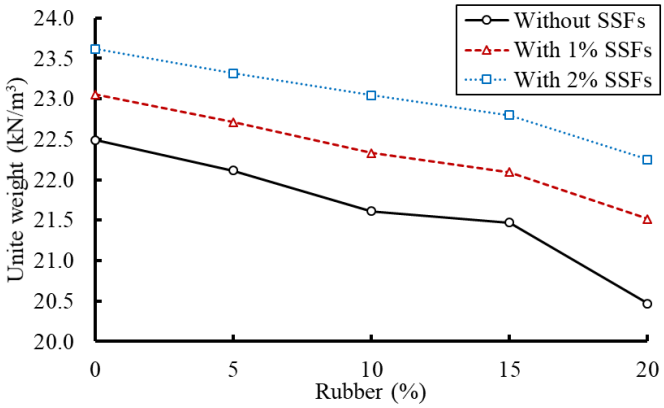

Figure 7. Effect of CR and SSFs on unit weight.

Figure 8 depicts the influence of temperature on the unit weight of rubberized concrete at the age of 28 days. The unit weights of the rubberized concrete were reduced by 7.6%, 7.2%, 6.8%, 6.6%, and 6.5% when the temperature increased for the concrete mixtures with CR content of 0%, 5%, 10%, 15%, and 20%, respectively. The mixture containing 20% CR displayed the least influence of temperature on the unit weight of the rubberized concrete when the temperature was less than 40 °C. However, the effect of elevated temperature on concrete with 20% CR became more pronounced after 40 °C. There was a slight increase in the mass losses of concrete with 20% CR compared to the other mixtures. Early mass loss was caused by the evaporation of free capillary and physically bounded moisture and the partial dehydration of the chemical compounds of the cement matrix [36]. Additionally, the decomposition of CR particles at elevated temperatures and the formation of voids in concrete due to the decomposition of these particles contributed to these reductions in unit weights [37,38]. The CR particles melted at a temperature of around 170 °C, which contributed to greater reductions in the unit weight due to the mass loss of the CR.

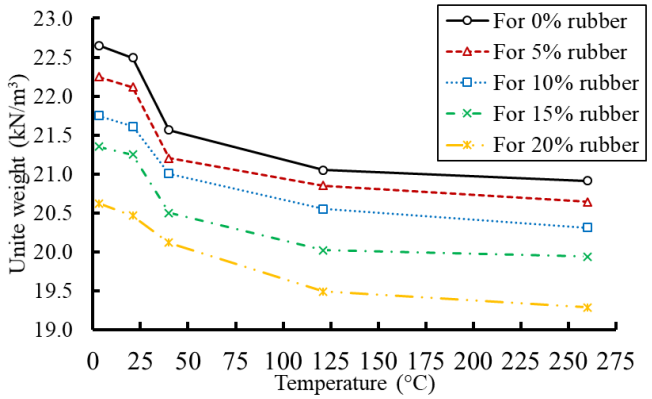

Figure 8. The unit weight of concrete with CR and exposed to temperature.

Two multinomial regression models were developed to explore the unit weight of concrete with CR, using experimental data at the age of 28 days. The goodness of fit measures and the coefficient of multiple determinations (R^2) was used to assess the adequacy of the proposed statistical regression models. Minitab statistical software V. 17 was used for model development.

The first regression model was developed to estimate the unit weight of hardened concrete with CR and SSFs, based on the volumetric content of the CR and SSFs. Equation (2) expresses this regression model:

$$UW = \gamma_c - 0.077R + 0.687F \quad (2)$$

where UW is the unit weight of the concrete mixture in kN/m^3, γ_c is the unit weight of the reference mixture, R is the volumetric content of rubber (%), and F is the volumetric content of SSFs (%). The adjusted R-squared was determined as R^2 = 95.92% for the regression model. Investigating the standardized coefficients of the model indicates that the rubber content has a negative impact on the unit weight of the mixture, which means that increasing the rubber content in the mixture will reduce the unit weight of the mixture. On the other hand, fiber content has a positive effect on the mixture's unit weight, meaning that an increase in the fiber content will increase the unit weight of the mixture.

Another multinomial regression model was developed to estimate the unit weight of hardened rubberized concrete under the effects of different temperatures. The temperature and CR content were used as predictive variables in the regression model (see Equations (3) and (4)).

$$UW = \gamma_c - 0.081R - 0.005T \quad (3\ ^\circ C \leq T \leq 21\ ^\circ C) \tag{3}$$

$$UW = \gamma_c - 0.1R - 0.005T \quad (21\ ^\circ C < T) \tag{4}$$

where UW is the unit weight of the concrete mixture in kN/m^3, γ_c is the unit weight of the reference mixture at the ideal temperature (21 °C), R is the CR content in the mixture (%), and T is the temperature in degree Celsius (°C). The adjusted R-squared value was determined as R^2 = 98.29% and 92.53%, respectively. Investigating the standardized coefficients of the model indicates that both predictive variables (i.e., rubber content and temperature) have a negative impact on the unit weight of the mixture (similar to the previous model). This means that the unit weight of the concrete mixture will decrease if the rubber content and temperature of the mixture increase. Comparisons between the experimental and prediction results are shown in Figure 9 to assess the adequacy of the proposed prediction model.

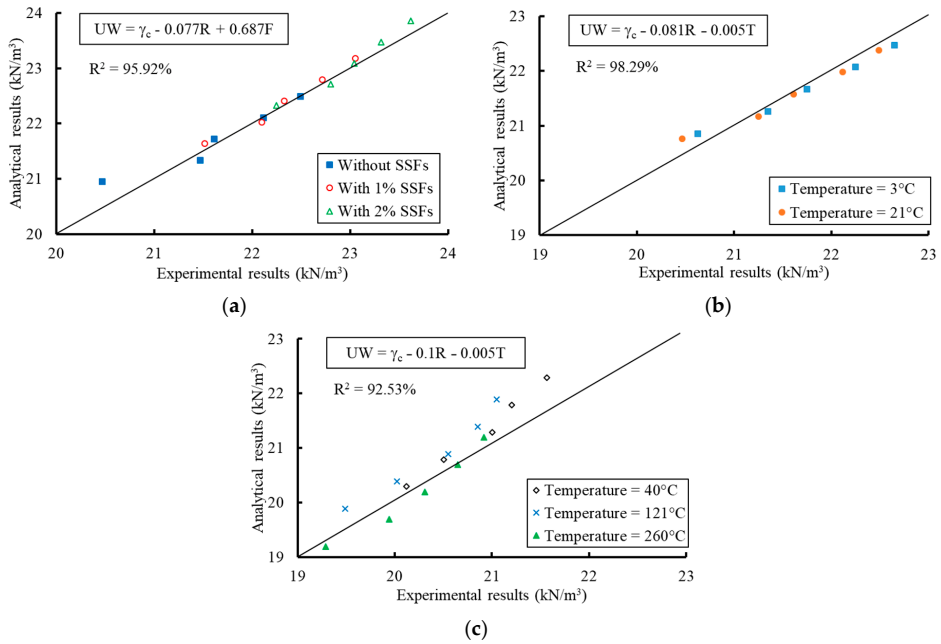

Figure 9. Regression between the experimental and analytical values of the unit weight. (**a**) Case of rubber content. (**b**) Case of rubber content and temperature (3 °C ≤ T ≤ 21 °C). (**c**) Case of rubber content and temperature (T > 21 °C).

3.3. Stress–Strain Relationships

The readings of the applied load and deflection were recorded during the compression tests, and subsequently, the stress–strain relationships were plotted. Figure 10 demonstrates the influence of CR content on stress–strain relationships. These relationships confirmed

reductions in concrete stiffness and compressive strength as the CR content increased. However, the ultimate strains increased with an increase in the CR content. The reason for these reductions was the lack of bond between the CR and the ingredients of concrete mix. The same conclusion was observed as the temperature increased (see Figure 11). In addition, the softening due to elevated temperature caused declination in the linear portion of the stress–strain relationships, and the curve became flattered where the slope of the ascending branch decreased.

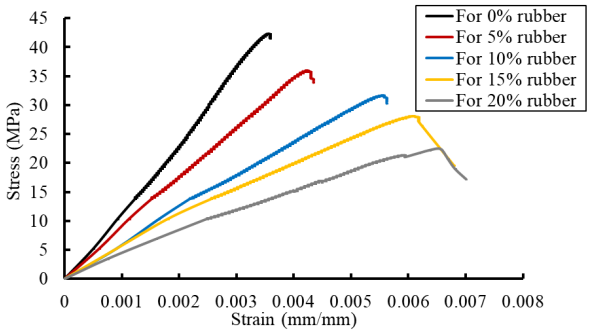

Figure 10. Effect of the CR content on the stress–strain relationships.

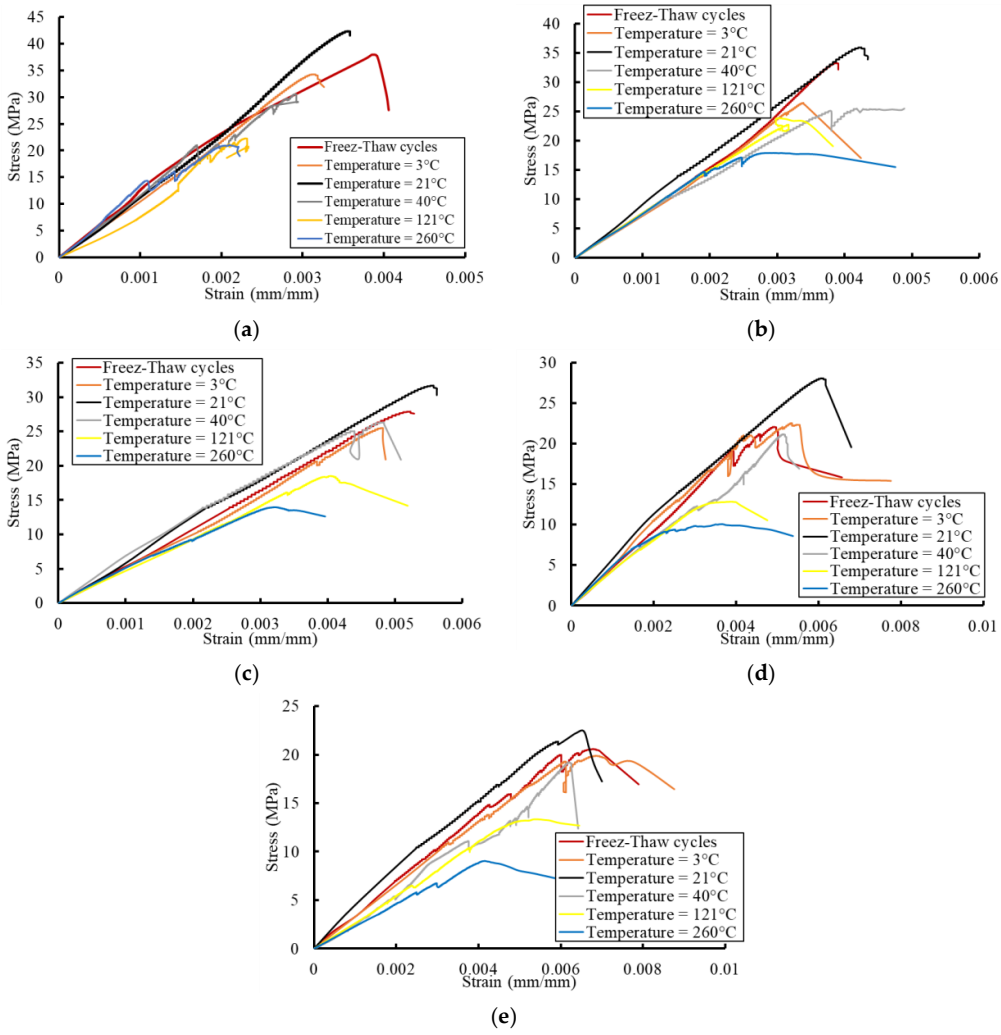

Figure 11. The stress–strain relationships of concrete with CR and exposed to temperatures. (**a**) 0% content of CR. (**b**) 5% content of CR. (**c**) 10% content of CR. (**d**) 15% content of CR. (**e**) 20% content of CR.

Conversely, the stiffness and compressive strength of the rubberized concrete specimens improved with the addition of SSFs. The improvement was enhanced as the percentage of SSFs increased, as shown in Figure 12. The SSFs were uniformly distributed and randomly oriented to arrest the micro-cracking mechanism and limit crack propagation.

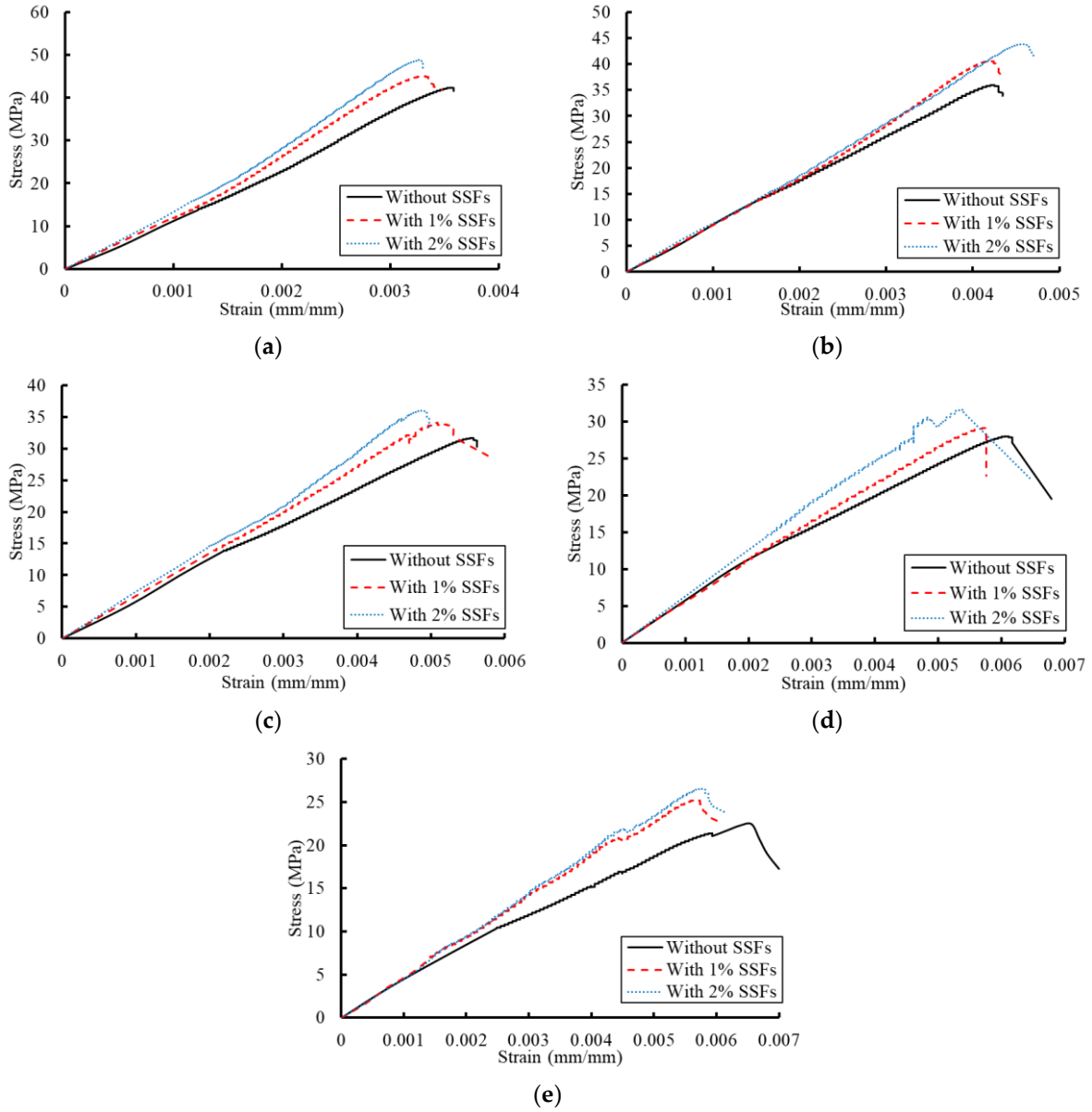

Figure 12. Effect of SSFs on the stress–strain relationships of rubberized concrete. (**a**) 0% content of CR. (**b**) 5% content of CR. (**c**) 10% content of CR. (**d**) 15% content of CR. (**e**) 20% content of CR.

3.4. Compressive Strength

Figure 13 shows the compressive strength of the tested specimens at different ages (3-, 7-, 14-, 28-, 56-, and 90-days). All concrete specimens with CR show adequate compressive strength at age 28 days, ranging from 21.7 MPa (for 20% of CR) to 37.2 MPa (for 5% of CR). The reductions in compressive strength ranged between 13% and 50%. The percentage of CR directly affected compressive strength, whereas a larger percentage of CR led to more drops in compressive strength. Similar rates of reduction were exhibited at different ages of concrete. Previous studies confirmed 10–59% reductions in the 28-age compressive strength [21]. The significant degradation in the adhesion between the cement paste and CR particles due to the smooth surfaces and softness of the CR particles increased the volume of

the weakest phase and interfacial transition zone [39]. Figure 14 demonstrates the influence of concrete age on the compressive strength of concrete with different CR content ratios. All concrete mixes gained more strength over time. However, the gain rate decreased as the CR content increased at the early age of concrete (age of 3 days). The modes of failure of concrete specimens with different CR contents are shown in Figure 15. The reference specimen without CR showed brittle and sudden failure, and cracks appeared throughout the entire surface. Numerous cracks were created as the CR percentage increased. The shape of failures for concrete specimens under compressive tests showed that with the increase in the CR percentage, the failure was accompanied by more crack propagations. Well-formed cones with vertical splitting were observed for concrete cylinders with 10% and 15% CR. Columnar vertical cracking was the mode of failure observed for 5% and 20% CR.

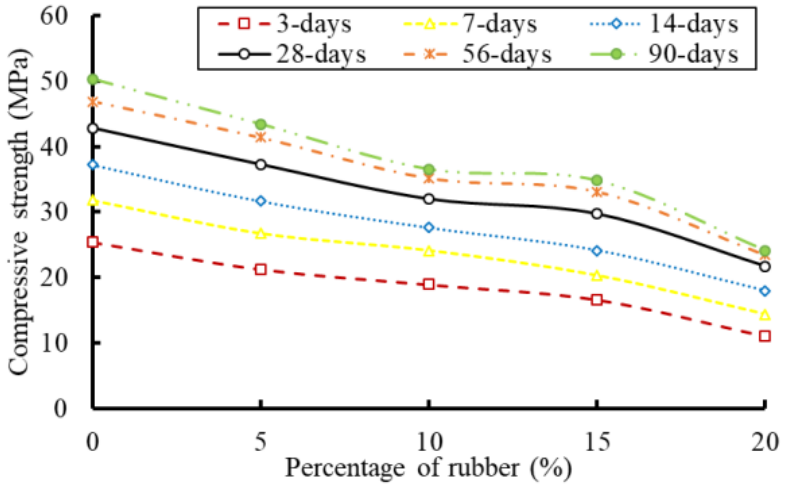

Figure 13. Effect of rubber content on compressive strength at different ages.

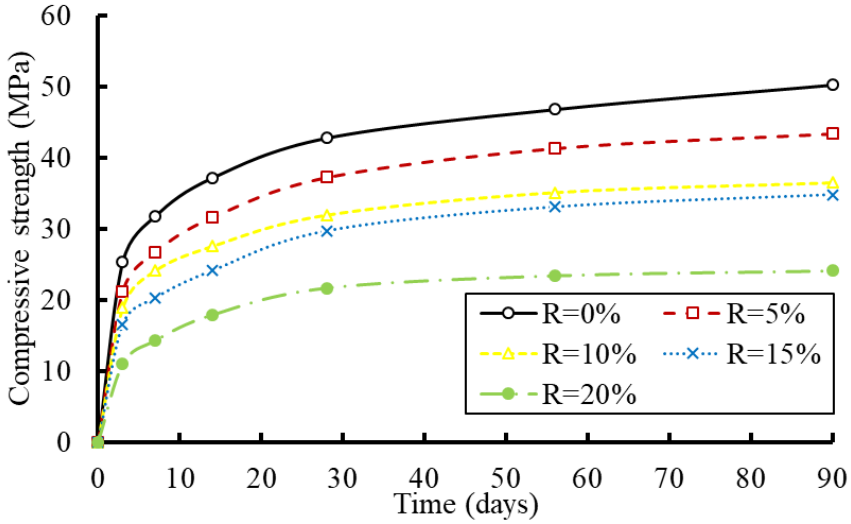

Figure 14. Effect of the concrete age on the compressive strength of concrete with different CR content ratios.

To compensate for these reductions in compressive strength, SSFs were added to the concrete mixes. Figure 16 shows the variations in strength after adding SSFs with CR to the concrete mixes. Slight improvements in compressive strength were obtained after using 1.0% and 2.0% SSF content without CR. However, a 33.3% enhancement in compressive strength was confirmed when using 2.0% SSFs with 20% CR content.

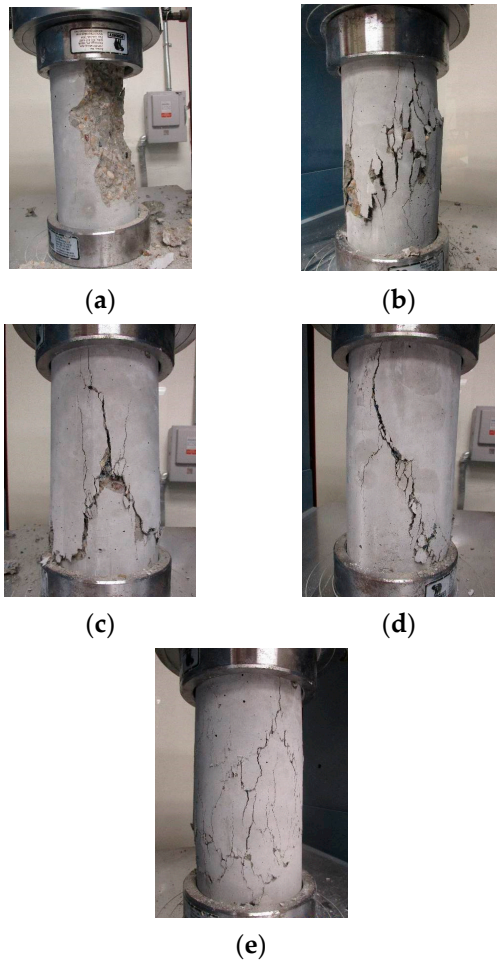

Figure 15. Modes of failure of concrete specimens with different CR contents. (**a**) 0% content of CR. (**b**) 5% content of CR. (**c**) 10% content of CR. (**d**) 15% content of CR. (**e**) 20% content of CR.

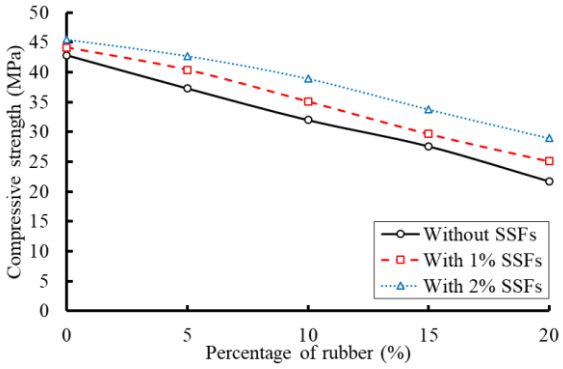

Figure 16. Effect of the SSF percentage on the compressive strength of concrete with CR.

The residual compressive strength of concrete containing CR after exposure to different temperatures (3 °C, 21 °C, 40 °C, 121 °C, and 260 °C) is shown in Figure 17. The specimens exposed to 21 °C achieved the highest compressive strength relative to those with the same CR content and under higher temperatures (see Figure 17). For the reference specimens without CR, the reductions in compressive strength were 19.4%, 26.5%, 43.2%, and 49.6% for the temperatures 3 °C, 40 °C, 121 °C, and 260 °C, respectively. However, these reductions were 9.2%, 8.8%, 40.4%, and 55.3% when the CR content was 20%. These results confirmed that the effect of cold and hot weather (3 °C and 40 °C) in reducing the compressive strength of concrete vanished as the CR content reached 20%. However, serious reductions were obtained at temperatures of 121 °C and 260 °C. The highest compressive strength for each

CR content was at a moderate temperature of 21 °C, and that strength reduced as the temperature increased (see Figure 18). At elevated temperatures, the early evaporation of free capillary and physically bounded moisture and partial dehydration of the chemical compounds of the cement matrix caused damage to the concrete surfaces [36], which were visually evaluated immediately after removal from the electric oven (see Figure 19). There was serious damage to the concrete surfaces of the specimens with 15% and 20% rubber content due to exposure to elevated temperatures of 121 °C and 260 °C, which led to serious reductions in concrete compressive strengths. The expansion of the CR inside the concrete mix, due to the elevated temperature, induced internal thermal stresses, which led to serious internal and external damage.

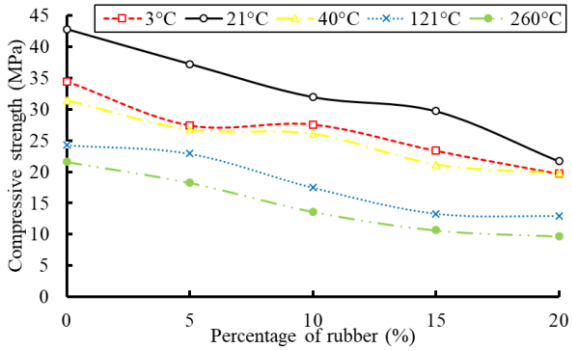

Figure 17. Effect of CR content on compressive strength at different temperatures.

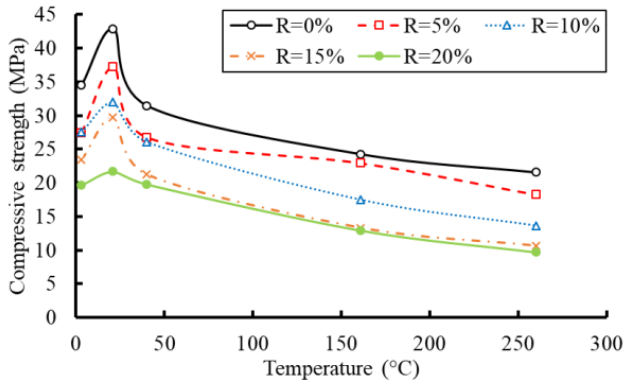

Figure 18. Effect of temperature on concrete with different percentages of CR.

15% CR content 20% CR content 15% CR content 20% CR content

(**a**) (**b**)

Figure 19. Serious damage to the concrete surface of specimens with 15% and 20% CR contents due to exposure to elevated temperatures of 121 °C and 260 °C. (**a**) For a temperature of 121 °C. (**b**) For a temperature of 260 °C.

The compressive strengths of rubberized concrete specimens after 28 freezing–thawing cycles were compared with the corresponding specimens without freezing–thawing cycles, as shown in Figure 20. There was a 17.6% reduction in compressive strength in the case of 0% CR content. However, this reduction decreased to 5.9% as the CR content increased to 20%. The addition of CR limited the side effects of freezing–thawing cycles on reducing the compressive strength of concrete.

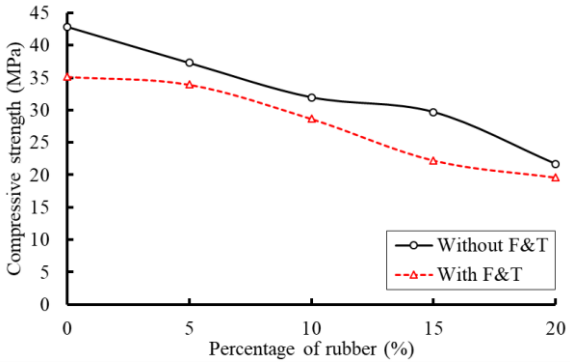

Figure 20. Effect of freezing–thawing cycles on the compressive strength of rubberized concrete.

A multinomial regression model was developed using the rubber and SSF volumetric contents to estimate the compressive strength. Equation (5) expresses the regression model:

$$CS = f_c^{'} - 0.9R + 2.65F \quad (5)$$

where CS is the compressive strength of concrete with CR and SSF contents (MPa), $f_c^{'}$ is the compressive strength of the reference concrete mix without CR and SSFs, R is the CR content in the mixture (%), and F is the SSF content in the mixture (%). The adjusted R-squared value was determined as R^2 = 98.19% percent. Another multinomial regression model was developed to explore the influence of CR content and temperature on the compressive strength of rubberized concrete mixtures. Equation (6) expresses the regression model:

$$CS = f_c^{'} - 0.09T - 0.9R \quad (6)$$

where CS is the compressive strength of rubberized concrete after exposure to temperature (MPa), R is the rubber content in the mixture (%), and T is the temperature in °C. The adjusted R-Squared of the developed regression model was determined as R^2 = 82.14% percent. Comparisons between the experimental and analytical results are shown in Figure 21.

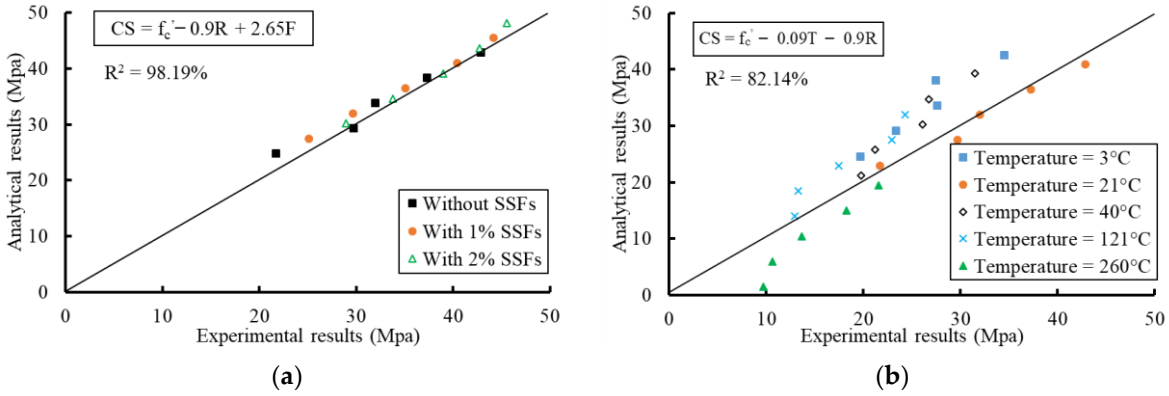

Figure 21. Regression between the analytical and experimental values of compressive strength. (**a**) The effect of CR content. (**b**) The effect of CR content and temperature.

3.5. Strain at Peak Stress

The strains corresponding to the peak stresses are demonstrated in Figure 22. The strains at peak stresses increased due to the effect of rubber. Moreover, more improvement in the ultimate strains was obtained as the CR content increased. The optimum ultimate strains were obtained at a temperature of 21 °C. However, these strains exhibited reductions as the temperature increased, and these reductions were more pronounced as the CR content increased. On the other hand, the SSFs decreased the strain of the rubberized concrete at peak stress. However, the addition of SSFs afforded a more prominent effect when the CR content exceeded 10%. For specimens without SSFs, the maximum increase in strain at the peak stress was approximately 85%, for a CR content of 20%. For specimens containing SSFs, the maximum increase in strain at peak stress was approximately 76%, for a CR content of 20%.

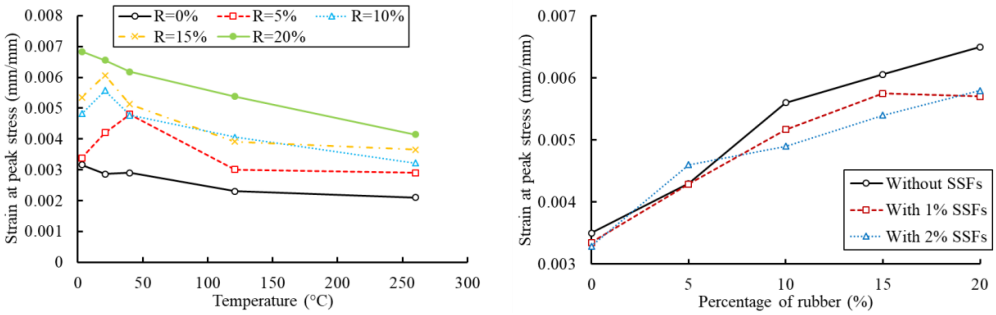

Figure 22. Strain at peak stress. (**a**) Effect of temperature. (**b**) Effect of SSFs.

3.6. Modulus of Elasticity

The modulus of elasticity, shown in Figure 23, was calculated by dividing the stress at 0.45fc′ by the respective strain recorded from compression tests. In general, replacing coarse aggregates with CR reduces the modulus of elasticity. For the 20% CR content, there was a 70.6% reduction in the modulus of elasticity. The modulus of elasticity and volumetric ratio of the coarse aggregate in concrete affect the modulus of elasticity of the resulting concrete [14]. The smaller the modulus of elasticity of the coarse aggregate, the weaker the concrete produced. Therefore, a higher volume of CR resulted in weaker concrete with a smaller modulus of elasticity. To compensate for this drop in the modulus of elasticity, SSFs were added to the concrete mix. After adding 2.0% SSF content, the modulus of elasticity was improved by 26.3% for concrete without CR. However, this improvement increased to 33.5% as the CR content increased to 20%. Moreover, the improvement in the modulus of elasticity due to increasing the SSF content from 1.0% to 2.0% decreased as the CR content increased. These improvements were 11.1% and 3.2% for the 0% and 20% CR contents, respectively.

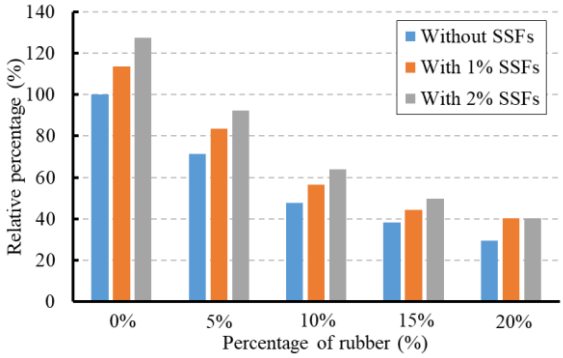

Figure 23. Modulus of elasticity of concrete with CR and SSFs normalized to the reference mix.

3.7. Compression Toughness

Figure 24 presents the effect of the CR percentage on the compression toughness of the tested specimens. Compression toughness, as defined in this study, is calculated as the area under the stress–strain relationship up to the ultimate strain value. These values indicate that the compression toughness improved with an increase in the CR content. Moreover, the compression toughness of rubberized concrete with SSFs was much improved relative to rubberized concrete without SSFs.

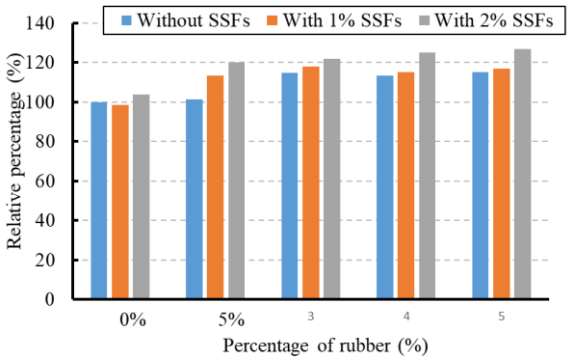

Figure 24. Compressive toughness of concrete with CR and SSFs normalized to the reference mix.

3.8. Indirect Tensile Strength

Figure 25 shows the results of the splitting tests after 28 days with respect to the CR and SSF contents. Reductions in the splitting tensile strength were observed after increasing the CR content. These reductions were 11.1%, 20.7%, 33.5%, and 43.5% for CR contents of 5%, 10%, 15%, and 20%, respectively. The very small cracks initiated between the CR particles and cement paste due to the weak bond holding them together were the main reason for these reductions [40,41]. Using SSFs in the concrete mix enhanced the indirect tensile strength by 29.2% and 43.1% when the percentages of the SSFs increased from 1.0% to 2.0%, respectively. Incorporating SSFs in rubberized concrete would bridge micro-cracks at an early age and enhance tensile strength [21].

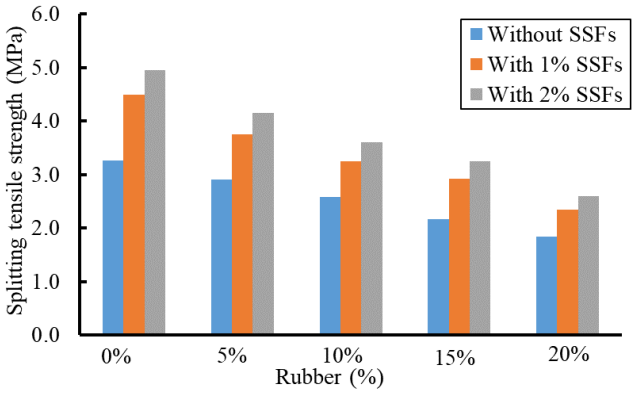

Figure 25. Results of the indirect tension tests.

3.9. Modulus of Rupture

Reductions in the modulus of rupture were obtained, as shown in Figure 26. These reductions ranged from 13.6% to 41.9% when the percentage of CR increased from 5% to 20%. Using 1.0% of the SSFs significantly enhanced the modulus of rupture by 5.7% to 14.5%, while the percentages of CR increased from 5% to 20%, respectively. Moreover, these improvements ranged from 15.9% to 33.3% in the case of the 2.0% SSFs.

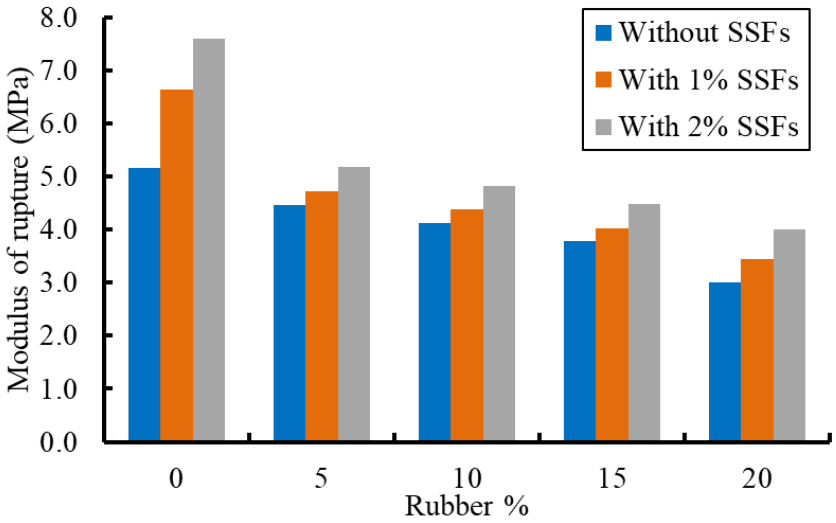

Figure 26. Bending test results (modulus of rupture).

4. Life Cycle Cost Analysis

To compute the long-term economic potentials of implementing rubberized concrete, a life cycle cost analysis (LCCA), which is a data-driven and systematic methodology, is used following these steps: (1) defining the application; (2) developing scenarios; (3) determining lifecycle cash flow streams; and (4) calculating net present values.

4.1. Application

Rubberized concrete has several applications, such as building facade systems and slabs, and roadway overlays (i.e., thin whitetopping (TWT)) [42]. In this research, TWT was selected as a potential application of rubberized concrete for the LCCA. TWT is a concrete overlay, generally, 101.6- to 177.8-mm, added to an existing asphalt concrete layer mainly constructed at the intersections, where shoving and rutting in asphalt pavement continue to cause problems [43]. TWT is mostly designed for a life span of 5 to 10 years.

4.2. Scenarios and the Expected Life Span of the Alternatives

Three scenarios, as listed in Table 2, are developed to compare the life cycle cost of rubberized concrete with the life cycle cost of ordinary concrete for roadway TWT application. Several research studies have illustrated that rubberized concrete mixtures offer a higher service life compared to ordinary concrete mixes. For instance, Liu et al. [44] confirmed that the toughness and cracking resistance of the concrete increased with an increase in rubber content (up to 20%) in the mixture. Moreover, the fatigue life and dynamic strain of rubberized concrete were better than those of ordinary concrete under certain stress levels [44]. Feng et al. [45] showed that adding CR to concrete mixtures enhanced the deformation capacity and crack resistance of the concrete. In this study, the same life spans are assumed for ordinary concrete mixtures and the rubberized concrete mixtures in the LCCA. A life span of 40 years is assumed for the roadway structure.

Table 2. Scenarios for implementing rubberized concrete and ordinary concrete in Texas, U.S.

Scenario	Overly Thickness (mm)	Life Cycle (Yrs.)	Analysis Period (Yrs.)
1	101.6 (4 in.)	5	40
2	127.0 (5 in.)	7	
3	177.8 (7 in.)	10	

4.3. Material Costs and Cashflow Streams

Agency costs for roadways include land achievement, construction, financing, maintenance, and operations [46]. In this study, TWT is assumed to be the resurfacing and

rehabilitation approach for roadway systems with a lifespan of 40 years. It is assumed that all agency costs, except the concrete mix cost for TWT, will be the same for the roadway system. Therefore, they are removed from the life cycle cost analysis. Table 3 presents the costs of the different concrete mixtures and their ingredients. The average of individual bid items used in highway maintenance projects in Texas [43] was used as the unit cost of the mixture ingredients.

Table 3. The unit cost of different concrete mixtures and their ingredients.

CR Content	Ingredients					Total ($/m^3)
	Cement ($0.29/kg)	Sand ($0.05/kg)	Gravel ($0.13/kg)	Water ($0.01/Lit)	Rubber ($0.22/kg)	
0%	$63.42	$37.01	$163.88	$2.44	$-	$266.75
5%	$63.42	$37.01	$155.64	$2.44	$7.94	$266.45
10%	$63.42	$37.01	$147.53	$2.44	$16.09	$266.49
15%	$63.42	$37.01	$139.16	$2.44	$23.81	$265.84
20%	$63.42	$37.01	$131.05	$2.44	$31.75	$265.67

In Texas, the first TWT was constructed at the intersection of Interstate Highway 20 and BU 83 in Abilene, Texas [47]. This intersection was selected as an illustration to conduct the LCCA of the TWT using rubberized concrete and to compare it with ordinary concrete. This project included a lane at the intersection with a width of 3.65 m (12 ft.) wide and a length of 53.3 m (175 ft.), which was covered by TWT. Table 4 presents the quantity and cost of concrete mixtures required for different TWT scenarios at the intersection. Figure 27 presents the cash flow streams for the TWT of the roadway using both ordinary concrete and rubberized concrete for all scenarios. This figure shows the time intervals for TWT with different thicknesses.

Table 4. Quantity and cost of concrete mixtures required for different TWT scenarios.

Scenario	Thickness	CR Content	Quantity	Project Material Cost
1	101.6 mm (4 in.)	0%	$3.65 * 53.3 * 0.1016$ 19.76 m^3	$5270.98
		5%		$5265.05
		10%		$5265.84
		15%		$5253.00
		20%		$5249.64
2	127.0 mm (5 in.)	0%	$3.65 * 53.3 * 0.127$ 24.70 m^3	$6588.73
		5%		$6581.32
		10%		$6582.30
		15%		$6566.25
		20%		$6562.05
3	177.8 mm (7 in.)	0%	$3.65 * 53.3 * 0.1778$ 34.59 m^3	$9226.88
		5%		$9216.51
		10%		$9217.89
		15%		$9195.41
		20%		$9189.53

4.4. Net Present Value (NPV)

To compare the life cycle cost of different concrete mixtures for the resurfacing of the intersection over the roadway's life span, the net present value (*NPV*) is used. This value is calculated as presented in Equation (7).

$$NPV = \sum_{t=0}^{n} \frac{Cashflow_t}{(1+i)^t} \quad (7)$$

where $Cashflow_t$ = concrete mixture cost at time t; i = discount rate; and n = life span of the roadway. A 1.5% discount rate is used in this analysis, as recommended by the U.S. Office of Management and Budget [48], for projects longer than 30 years.

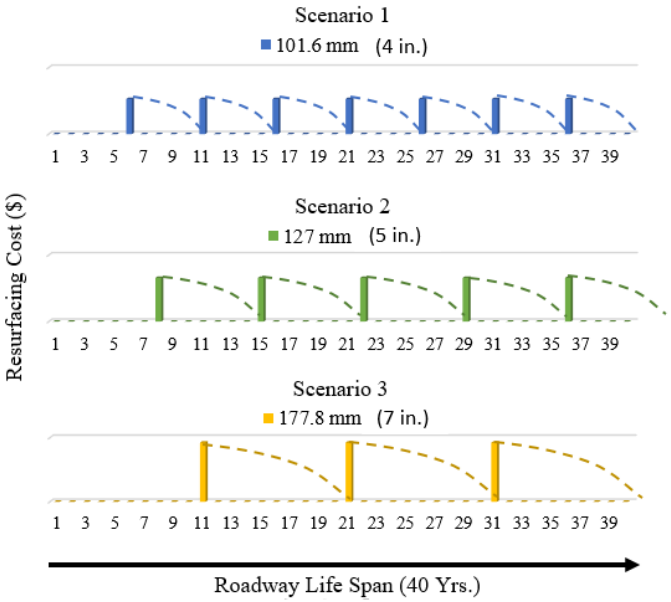

Figure 27. Cashflow streams for TWT over a 40-year life span of the roadway using both ordinary concrete and rubberized concrete for different scenarios.

Figure 28 illustrates the *NPV* of all concrete mixtures for the three scenarios. Comparing all the *NPV*s for different scenarios shows that using rubberized concrete mixtures for TWT offers slightly lower *NPV*s compared to the ordinary concrete mix. Among the rubberized concrete mixtures, RC-20 offers the lowest *NPV*s (i.e., \$27,179.60, \$23,903.57, and \$20,315.60) for all three scenarios (i.e., 101.6 mm, 127 mm, and 177.8 mm) due to having higher percentages of CR as a cheaper aggregate substitute in the mixture. Comparing the scenarios reveals 177.8 mm (7 in.) is a cost-efficient option for TWT at this location. It is noteworthy to mention that only material costs were considered in this study. The benefits of using rubberized concrete are beyond the cost of materials. Rubberized concrete offers several advantages over ordinary concrete. The unit weight of rubberized concrete was lower than that of the ordinary concrete mixture. This can increase labor productivity in handling the mixture. Rubberized concrete also provides excellent freeze–thaw durability compared to ordinary concrete mixtures [49]. The improved fatigue life of the rubberized concrete relative to conventional concrete makes the rubberized mixture a better solution for roadway applications. Finally, rubberized concrete mixtures have fewer negative environmental impacts compared to ordinary concrete mixtures.

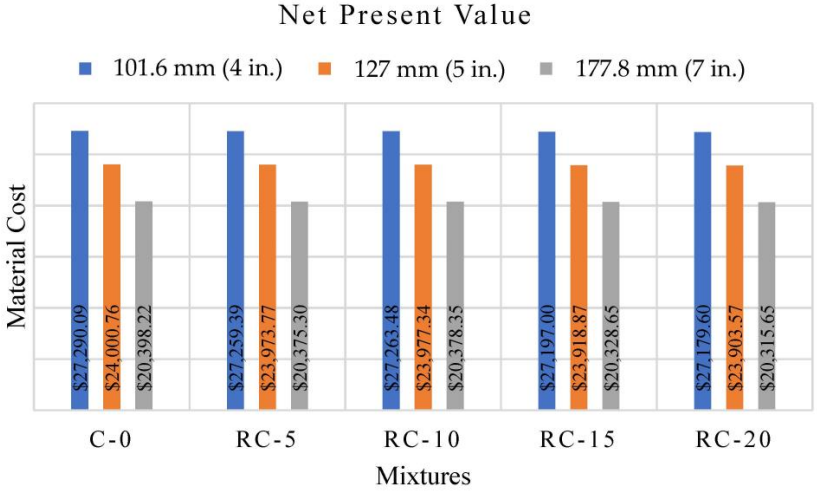

Figure 28. Net present values of implementing different concrete mixtures for TWT at the intersection.

5. Conclusions

In this paper, concrete specimens were prepared with different percentages of rubber (0%, 5%, 10%, 15%, and 20%). Other parameters, such as freezing–thawing cycles, temperature, and SSFs, were also investigated. The workability of fresh concrete and the compression properties of hardened concrete were examined. An LCCA to identify and quantify the possible benefits of using CR in concrete mixes was carried out. The main conclusions of this study are as follows.

- Increasing the percentage of CR resulted in reducing the slump of concrete, especially when 20% rubber was used. Additional reductions in the slump were obtained when SSFs were used in the concrete mixes, and these reductions increased as the content of SSFs increased. Slump decreased by approximately 30% when 20% rubber was used (without SSFs). However, using 1.0% and 2.0% of the SSFs with 20% rubber caused reductions in the slump value of nearly 45% and 55%, respectively.
- The average unit weight decreased by 1.3%, 2.5%, 3.4%, and 5.7% of the control mixture when 5%, 10%, 15%, and 20% of the CR were incorporated into the concrete mixtures, respectively. A similar trend was observed for mixtures with the same replacement ratios when CR was added to SSF concrete.
- The unit weights of the rubberized concrete were reduced when the temperature increased, and this reduction decreased as the CR content increased. The mixture containing 20% CR displayed the lowest effect of temperature on the unit weight of the rubberized concrete.
- The stress–strain relationships confirmed reductions in the concrete stiffness and compressive strength with an increase in the CR content. However, the ultimate strains increased with an increase in the CR content. On the other hand, the stiffness and compressive strength of the rubberized concrete specimens improved with the addition of SSFs. The improvement was enhanced as the content of SSFs increased.
- All concrete mixes gained more strength over time. However, the gaining rate decreased as the CR content increased at the early age of concrete (age of 3-day).
- The compressive strength reductions ranged between 13% and 50% based on the percentage of CR in the concrete mix. Slight improvements in compressive strength were obtained after using 1.0% and 2.0% SSF content without CR. However, a 33.3% improvement in compressive strength was confirmed when using 2.0% SSFs with 20% CR content. The contribution of the SSFs in enhancing compressive strength increased as the CR content increased.
- The effect of cold and hot weather (3 °C and 40 °C) in reducing the compressive strength of concrete vanished as the CR content reached 20%. However, serious reductions were obtained at temperatures of 121 °C and 260 °C.
- Reductions in the splitting tensile strength were observed after increasing the CR content. The tensile strength decreased by 11.1%, 20.7%, 33.5%, and 43.5% for CR contents of 5%, 10%, 15%, and 20%, respectively. However, using SSFs in the concrete mix enhanced the indirect tensile strength by 29.2% and 43.1% when the percentages of SSFs increased from 1.0% to 2.0%, respectively.
- Using rubberized concrete mixtures for thin whitetopping offered a slightly lower *NPV* compared to the ordinary concrete mix. Among the rubberized concrete mixtures, RC-20 offered the lowest *NPV*s for all three scenarios (i.e., 101.6 mm, 127 mm, and 177.8 mm) due to having higher percentages of CR as a cheaper aggregate substitute in the mixture.

Author Contributions: Conceptualization, A.E.-Z. and P.M.; methodology, A.E.-Z.; software, B.A.; validation, A.E.-Z., M.S. and B.A.; formal analysis, A.E.-Z.; investigation, A.E.-Z. and M.S.; resources, M.S.; data curation, A.E.-Z.; writing—original draft preparation, A.E.-Z. and B.A.; writing—review and editing, A.E.-Z. and B.A.; visualization, P.M.; supervision, A.E.-Z., B.A. and P.M. All authors have read and agreed to the published version of the manuscript.

Funding: This research received no external funding.

Institutional Review Board Statement: Not applicable.

Informed Consent Statement: Not applicable.

Data Availability Statement: Not applicable.

Acknowledgments: The research described in this paper was financially supported by the Texas A&M University-Commerce Undergraduate Grant Program at Texas A&M University-Commerce.

Conflicts of Interest: The authors declare no conflict of interest.

References

1. Lewis, G. *"Impacts & Results In your Region", Regional Solid Waste Grants Program Funding Report Fiscal Years 2014/2015*; Texas Association of Regional Councils: Austin, TX, USA, 2016.
2. Mhaya, A.M.; Huseien, G.F.; Abidin, A.R.Z.; Ismail, M. Long-term mechanical and durable properties of waste tires rubber crumbs replaced GBFS modified concretes. *Constr. Build. Mater.* **2020**, *256*, 119505. [CrossRef]
3. Hasan, A.; Dincer, I. Comparative assessment of various gasification fuels with waste tires for hydrogen production. *Int. J. Hydrog. Energy* **2019**, *44*, 18818–18826. [CrossRef]
4. Habib, A.; Yıldırıma, U. Prediction of the dynamic properties in rubberized concrete. *Comput. Concr.* **2021**, *27*, 185–197. [CrossRef]
5. Siringi, G.; Abolmaali, A.; Aswath, P.B. Properties of concrete with tire-derived aggregate partially replacing coarse aggregates. *Sci. World J.* **2015**, *2015*, 863706. [CrossRef]
6. Batayneh, M.K.; Marie, I.; Asi, I. Promoting the use of crumb rubber concrete in developing countries. *Waste Manag.* **2008**, *28*, 2171–2176. [CrossRef]
7. Panda, K.; Parhi, P.; Jena, T. Scrap-Tyre-Rubber replacement for aggregate in cement concrete: Experimental study. *Int. J. Earth Sci. Eng.* **2012**, *5*, 1692–1701.
8. Padhi, S.; Panda, K.C. Fresh and hardened properties of Rubberized Concrete using fine rubber and silpozz. *Adv. Concr. Constr.* **2016**, *4*, 49–69. [CrossRef]
9. Al-Tayeb, M.M.; Abu Bakar, B.H.; Akil, H.M.; Ismail, H. Performance of rubberized and hybrid rubberized concrete structures under static and impact load conditions. *Exp. Mech.* **2013**, *53*, 377–384. [CrossRef]
10. Guo, J.; Huang, M.; Huang, S.; Wang, S. An Experimental Study on Mechanical and Thermal Insulation Properties of Rubberized Concrete Including its Microstructure. *Appl. Sci.* **2019**, *9*, 2943. [CrossRef]
11. Chen, Z.; Li, L.; Xiong, Z. Investigation on the interfacial behaviour between the rubber-cement matrix of the rubberized concrete. *J. Clean. Prod.* **2019**, *209*, 1354–1364. [CrossRef]
12. Xiong, Z.; Tang, Z.; He, S.; Fang, Z.; Chen, Z.; Liu, F.; Li, L. Analysis of mechanical properties of rubberised mortar and influence of styrene–butadiene latex on interfacial behaviour of rubber–cement matrix. *J. Constr. Build. Mater.* **2021**, *300*, 124027. [CrossRef]
13. Ling, T. Prediction of density and compressive strength for rubberized concrete blocks. *Constr. Build. Mater.* **2011**, *25*, 4303–4306. [CrossRef]
14. Al-Dala'ien, R.N.S. An Assessment of Mechanical Properties of Using Tires Rubber as a Partial Replacement of Aggregate in Sustainable Concrete. *J. Green Eng.* **2020**, *10*, 5017–5033.
15. Gul, M.; Qasab, R.A. Effect of Tyre Rubber on the Mechanical Properties of Concrete. *J. Emerg. Technol. Innov. Res.* **2018**, *5*, 658–664.
16. Feng, W.; Liu, F.; Yang, F.; Li, L.; Jing, L. Experimental study on dynamic split tensile properties of rubber concrete. *J. Constr. Build. Mater.* **2018**, *165*, 675–687. [CrossRef]
17. Güneyisi, E.; Gesoğlu, M.; Mermerdaş, K.; İpek, S. Experimental investigation on durability performance of Rubberized Concrete. *Adv. Concr. Constr.* **2014**, *2*, 193–207. [CrossRef]
18. Karimipour, A.; Ghalehnovi, M.; Brito, J. Mechanical and durability properties of steel fiber-reinforced rubberised concrete. *Constr. Build. Mater.* **2020**, *257*, 119463. [CrossRef]
19. Liu, F.; Chen, G.; Li, L.; Guo, Y. Study of impact performance of rubber reinforced concrete. *J. Constr. Build. Mater.* **2012**, *36*, 604–616. [CrossRef]
20. Eisa, A.S.; Shehab, H.K.; El-Awady, K.A.; Nawar, M.T. Improving the flexural toughness behavior of R.C beams using micro/nano silica and steel fibers. *Adv. Concr. Constr.* **2020**, *11*, 45–58. [CrossRef]
21. Eisa, A.S.; Elshazli, M.T.; Nawar, M.T. Experimental investigation on the effect of using crumb rubber and steel fibers on the structural behavior of reinforced concrete beams. *Constr. Build. Mater.* **2020**, *252*, 119078. [CrossRef]
22. Ahmad, S.; Umar, A.; Masood, A.; Nayeem, M. Performance of self-compacting concrete at room and after elevated Temperature incorporating Silica fume. *Adv. Concr. Constr.* **2019**, *7*, 31–37. [CrossRef]
23. Salhi, M.; Li, A.; Ghrici, M.; Bliard, C. Effect of Temperature on the behavior of self-compacting concretes and their durability. *Adv. Concr. Constr.* **2019**, *7*, 277–288. [CrossRef]
24. Pokorný, J.; Záleská, M.; Pavlíková, M.; Pavlík, Z. The Influence of Elevated Temperatures on Thermal Properties of Concrete with Crumb Rubber. In *AIP Conference Proceedings*; AIP Publishing LLC: Melville, NY, USA, 2019; Volume 2293, pp. 070003-1–070003-4. [CrossRef]

25. Bengar, H.A.; Shahmansouri, A.A.; Sabet, N.A.Z.; Kabirifar, K.; Tam, V.W.Y. Impact of elevated temperatures on the structural performance of recycled rubber concrete: Experimental and mathematical modeling. *Constr. Build. Mater.* **2020**, *255*, 119374. [CrossRef]
26. Mousavimehr, M.; Nematzadeh, M. Predicting post-fire behavior of crumb rubber aggregate concrete. *Constr. Build. Mater.* **2019**, *229*, 116834. [CrossRef]
27. Grinys, A.; Augonis, A.; Daukšys, M.; Pupeikis, D. Mechanical properties and durability of rubberized and SBR latex modified rubberized concrete. *Constr. Build. Mater.* **2020**, *248*, 118584. [CrossRef]
28. Luo, T.; Zhang, C.; Sun, C.; Zheng, X.; Ji, Y.; Yuan, X. Experimental Investigation on the Freeze–Thaw Resistance of Steel Fibers Reinforced Rubber Concrete. *Materials* **2020**, *13*, 1260. [CrossRef]
29. *ASTM C150/C150M-20*; Standard Specification for Portland Cement. ASTM International: West Conshohocken, PA, USA, 2020.
30. *ASTM C31/C31M-19a*; Standard Practice for Making and Curing Concrete Test Specimens in the Field. ASTM International: West Conshohocken, PA, USA, 2019.
31. *ASTM C39/C39M-20*; Standard Test Method for Compressive Strength of Cylindrical Concrete Specimens. ASTM International: West Conshohocken, PA, USA, 2020.
32. *ASTM C496/C496M-17*; Standard Test Method for Splitting Tensile Strength of Cylindrical Concrete Specimens. ASTM International: West Conshohocken, PA, USA, 2017.
33. *ASTM, C293/C293M-16*; Standard Test Method for Flexural Strength of Concrete (Using Simple Beam with Center-Point Loading). ASTM International: West Conshohocken, PA, USA, 2016.
34. *ASTM C143/C143M-15a*; Standard Test Method for Slump of Hydraulic Cement Concrete. ASTM International: West Conshohocken, PA, USA, 2015.
35. Zhang, Z.; Ma, H.; Qian, S. Investigation on properties of ECC incorporating crumb rubber of different sizes. *J. Adv. Concr. Technol.* **2015**, *13*, 241–251. [CrossRef]
36. Ahmad, J.; Zhou, Z.; Majdi, A.; Alqurashi, M.; Deifalla, A.F. Overview of Concrete Performance Made with Waste Rubber Tires: A Step toward Sustainable Concrete. *Materials* **2022**, *15*, 5518. [CrossRef]
37. Correia, J.; Marques, A.M.; Pereira, C.M.C.; de Brito, J. Fire reaction properties of concrete made with recycled rubber aggregate. *J. Fire Mater.* **2012**, *36*, 139–152. [CrossRef]
38. Marques, A.; Correia, J.; De Brito, J. Post-fire residual mechanical properties of concrete made with recycled rubber aggregate. *J. Fire Saf.* **2013**, *58*, 49–57. [CrossRef]
39. Poon, C.S.; Shui, Z.H.; Lam, L. Effect of microstructure of ITZ on compressive strength of concrete papered with recycled aggregates. *Constr. Build. Mater.* **2004**, *18*, 461–468. [CrossRef]
40. Sofi, A. Effect of waste tyre rubber on mechanical and durability properties of concrete—A review. *Ain Shams Eng. J.* **2017**, *9*, 2691–2700. [CrossRef]
41. Li, G.; Stubblefield, M.A.; Garrick, G.; Eggers, J.; Abadie, C.; Huang, B. Development of waste tire modified concrete. *Cem. Concr. Res.* **2004**, *34*, 2283–2289. [CrossRef]
42. Texas Department of Transportation (TxDOT). 2021; Pavement Manual. Available online: http://onlinemanuals.txdot.gov/txdotmanuals/pdm/manual_notice.htm (accessed on 29 June 2021).
43. Texas Department of Transportation (TxDOT). 2021; Average Low Bid Unit Prices-Highway Maintenance Projects. Available online: https://www.txdot.gov/business/letting-bids/average-low-bid-unit-prices.html (accessed on 13 October 2021).
44. Liu, F.; Zheng, W.; Li, L.; Feng, W.; Ning, G. Mechanical and fatigue performance of rubber concrete. *Constr. Build. Mater.* **2013**, *47*, 711–719. [CrossRef]
45. Feng, W.; Chen, B.; Yang, F.; Liu, F.; Li, L.; Jing, L.; Li, H. Numerical study on blast responses of rubberized concrete slabs using the Karagozian and Case concrete model. *J. Build. Eng.* **2021**, *33*, 101610. [CrossRef]
46. Hicks, R.G.; Lundy, J.R.; Epps, J.A. *Life Cycle Costs for Asphalt-Rubber Paving Materials*; Rubber Pavements Association: Tempe, AZ, USA, 1999.
47. Zhou, W.; Won, M.; Choi, P. Performance Evaluation of Whitetopping with Improved Design Practices in Texas. *J. Test. Eval.* **2018**, *47*, 2127–2149. [CrossRef]
48. U.S. Office of Management and Budget. Discount Rates for Cost-Effectiveness, Lease Purchase, and Related Analyses. Circular A-94; National Institute of Building Sciences: Washington, DC, USA, 2016.
49. Wang, J.; Dai, Q.; Si, R.; Ma, Y.; Guo, S. Fresh and mechanical performance and freeze-thaw durability of steel fiber-reinforced rubber self-compacting concrete (SRSCC). *J. Clean. Prod.* **2020**, *277*, 123180. [CrossRef]

Disclaimer/Publisher's Note: The statements, opinions and data contained in all publications are solely those of the individual author(s) and contributor(s) and not of MDPI and/or the editor(s). MDPI and/or the editor(s) disclaim responsibility for any injury to people or property resulting from any ideas, methods, instructions or products referred to in the content.